Sensors and Actuators B 210 (2015) 649–655

Contents lists available at ScienceDirect

Sensors and Actuators B: Chemical

journal homepage: www.elsevier.com/locate/snb

# Detection of ion adsorption at solid–liquid interfaces using internal reflection ellipsometry

Lei Wang, Cunlu Zhao, Michel H.G. Duits, Frieder Mugele, Igor Siretanu*

*Physics of Complex Fluids Group and MESA+ Institute, Faculty of Science and Technology, University of Twente, PO Box 217, 7500AE Enschede, The Netherlands*

ARTICLE INFO

*Article history:*
Received 9 July 2014
Received in revised form
17 December 2014
Accepted 18 December 2014
Available online 12 January 2015

*Keywords:*
Internal reflection ellipsometry
Ion adsorption
Electric double layer
Surface complexation reactions

ABSTRACT

We use imaging internal reflection ellipsometry (IRE) in combination with a microfluidic device to study the adsorption of inorganic salt ions to silica–water interfaces. In our data analysis, the measured polarization-dependent reflectivity is compared to calculations from a layer stack model, where the electric double layer is modeled as a separate layer. Due to the high resolution of our technique, we are able to quantify the adsorption of $Na^+$ and $Ca^{2+}$ ions from aqueous solutions of their chloride salts as a function of their bulk concentrations at pH 3 and 10. Our measurements demonstrate a preferential adsorption of $Ca^{2+}$ counterions. The experimental results are well described by calculations using a triple layer surface complexation model for the electric double layer with published equilibrium constants.



## 1. Introduction

Changes of surface structure and function upon adsorption have important consequences in many fields such as lubrication [1], catalysis [2,3], oil recovery [4], drug delivery [5], nuclear waste disposal [6], *etc.* Among these applications, the silicate mineral-water system is particularly important because many chemical processes in the aquatic ecosystem occur on mineral surfaces in the presence of organic or inorganic molecules. Experimental studies have shown that ions, in particular divalent ions, can serve as a bridge to stabilize organic molecules both at solid/liquid [7–11] and liquid/liquid interfaces [12]. Some of these findings have important implications for industry, like the low salinity water flooding process in enhanced oil recovery [13–16]. Despite numerous studies, the interactions between ions and solid surfaces are still incompletely understood. They are the result of a complex interplay, involving chemical and structural changes, as well as a dynamics that includes not only the adsorption reaction but also the competition and exchange of ions and correlations amongst them. Ambient conditions such as pH, ionic strength, the presence of competing or promoting ions as well as the nature and the amount of substrate, also have significant effects on the distribution of cations and anions over the solid–solution interface [17].

Many approaches, both experimental and computational, have been developed to understand adsorption phenomena. Classical potentiometric titration [18] and streaming potential measurements [19] are widely used for characterizing ion adsorption to solid substrates. And the results have been compared with predictions from competing theoretical approaches such as surface complexation models (SCM) [20], density functional theory (DFT) [25], Monte Carlo (MC) [21,22] and molecular dynamics (MD) simulations, and others [23]. Each of these theoretical approaches has its advantages and limitations. For example, SCM is unable to explain surface overcharging. Its application is limited to certain electrolytes or oxides at restricted ionic strengths and surface coverages. And the magnitudes of the equilibrium constants are not always transferable to experiments without corrections for differences in site density, capacitances and surface area. DFT is restricted by its use of very large surface unit cells, while MC and MD require a huge computational effort and are subjected to limitations in both the number of molecules they can deal with, and the time range over which the molecular system can be studied. More details can be found in detailed review of Rimola et al. [23]. Ellipsometry [24] and reflectometry [25] give insights into the distribution and adsorption of ions. Recent progress in atomic force microscopy (AFM) has provided the capability to study ion adsorption at the molecular scale, revealing complex and striking behaviors [26,27].

Compared to AFM, optical techniques have the advantage of being fast and non-intrusive, and they allow – under favorable conditions – chemically specific sensing and real-time signal processing. Specific methods such as surface plasmon resonance,

* Corresponding author. Tel.: +31 534893089; fax: +31 534891096.
*E-mail addresses:* siretanu_igor@yahoo.com, i.siretanu@utwente.nl (I. Siretanu).

http://dx.doi.org/10.1016/j.snb.2014.12.127
0925-4005/

reflectometry, and ellipsometry all possess a very high sensitivity that allows for the detection of fractions of monolayers of adsorbed organic or inorganic material—provided that adsorbate and ambient solution have sufficiently distinct optical properties. In the present work, we use ellipsometry to study the adsorption of ions from an aqueous solution to solid–liquid interfaces based on the changes in polarization state of the light upon reflection at the interface. In particular, we use ellipsometry in an imaging mode in combination with microfluidic channels that allow us to investigate several fluid compositions in parallel.

Common ellipsometry operates in "external" mode, the incident light comes from a low refractive index medium (air or liquid) to a higher one (a solid or liquid) implying that the light passes through the liquid phase. The latter aspect makes it difficult to combine with microfluidic channels. Therefore, we operate ellipsometry in internal reflection mode (so-called internal reflection ellipsometry (IRE)) which is hardly affected by microfluidic structures on the fluid side.

In this paper, we make use of an IRE setup to explore the effects of concentration, salinity, and pH on the adsorption behavior of mono- and divalent ions at silica–water interfaces. The amounts of adsorbed ions at different pH conditions are determined by fitting the ellipsometric angles using a suitable optical layer stack model. Finally, optical thickness of the ion adsorption layer extracted from the experiments is compared to predictions from a triple layer surface complexation model (SCM).

## 2. Experimental details

### 2.1. Materials

$CaCl_2{\cdot}2H_2O$ and NaCl (ACS reagent grade, Sigma Aldrich) and deionized water with a resistivity of 18.2 MΩ·cm (Synergy-UV, Millipore) were used to prepare the solutions. The pH was adjusted with HCl and NaOH standard solutions. BK-7 glass substrates with a deposited $Nb_2O_5$ layer (to enhance internal reflection) and an additional silica layer on top were purchased from ST Instruments. Before experiments, substrates were cleaned by rinsing with Millipore water, ethanol and isopropanol and gently dried with $N_2$. Then, samples were exposed to an air plasma treatment (Harrick Plasma) for 15 min. Roughness and morphology of the silica surface were assessed by AFM in tapping mode (Icon, Veeco). The surface is very smooth and reveals no spatial structure, with root-mean square roughness smaller than 0.4 nm (see the Supplementary information).

### 2.2. Methods

The measurements were carried out on a commercial imaging nulling-ellipsometer (EP3 Nanoscope, Accurion). The instrument is additionally equipped with an equilateral prism and a home-made microfluidic cell which enables parallel measurements under flow injection conditions. For liquid handling, a peristaltic pump (REGLO Digital MS-2/12) was used. Using the vacuum induced by the pump, solutions are carefully sucked into the cell, to avoid the formation of air-bubbles. A laser beam ($\lambda = 658$ nm) first passes through a polarizer and is then refracted into the prism, which provides coupling of the light beam into the layer of $Nb_2O_5$. The silica layer is exposed to an aqueous solution that is flushed through the microfluidic channel, as shown in Fig. 1a. Close to the Brewster angle, the reflectivity is very sensitive to the presence of thin adsorbed layers at the solid–liquid interface and the angle $\Psi$ displays a minimum, as shown in Fig. 1b. IRE measures the polarization changes of the reflected light, expressed in terms of $\Psi$ and $\Delta$. Optical properties of samples can be obtained by inserting these two parameters in Fresnel's equation [28].

**Table 1**
Layer stack model for IRE data analysis.

| Layer | Parameters | Comments |
|---|---|---|
| 4. BK-7 glass | $n = 1.515$, $k = 0$ | Fixed during fitting |
| 3. $Nb_2O_5$ | $n = 2.310$, $k = 0$<br>$d$: 70–80 nm | The values of d are obtained by fitting IRE data for every new sample, then both of them are kept fixed for further fittings. |
| 2. $SiO_2$ | $n = 1.456$, $k = 0$<br>$d$: 15–25 nm | |
| 1. Adsorbed layer* | $n_a$ and $d_a$ to be determined | |
| 0. Water** | $n = 1.332$, $k = 0$ | Fixed during fitting |

*Note:* all optical parameters are at wavelength 658 nm.
* For the measurement with water in the flow cell, this layer is not included in the model; in the analysis of adsorbed layer, region of $n_a$ is fixed between 1 and 2, $d_a$ can be fixed anywhere between 0.5 nm and 5 nm, see the discussion for details.
** When other salt solutions are used, $n_{bulk}$ is obtained by fitting IRE data.

To achieve the highest sensitivity, one first has to find the critical angle from the dependence of the ellipsometric angles on the Angle of Incidence (AOI). This is done under static conditions (*i.e.* no flow) with deionized water in the flow cell. The $\Psi$ and $\Delta$ angles are recorded in the AOI range from 48° to 56°, the AOI is varied in steps of 0.2° (Fig. 1b). At the minimum of $\Psi_0$, $\Delta_0$ displays a maximum slope (Fig. 1b). This is the condition of optimum sensitivity. Fig. 1b also shows the upward shift of the $\Psi$ and $\Delta$ *vs.* AOI curves by approximately 1° for a 1 M $CaCl_2$ solution (magenta) as compared to pure water (olive). Experimentally, we can detect shifts of $\Psi$ and $\Delta$ down to approximately 0.01° and 0.05°, respectively. To extract the optical properties, the sample (including adsorbed layer) is represented by a one-dimensional layer stack (see Fig. 2c). Each layer $i$ is characterized by its thickness $d_i$ and its refractive index $n_i$ (see Table 1). For the glass substrate, the $Nb_2O_5$ layer and the $SiO_2$ layer, these properties are calibrated in initial measurements with pure water. Subsequently, the properties of these layers are kept fixed in the analysis of the $\Psi$ and $\Delta$ curves obtained during the ion adsorption measurements at variable fluid compositions. The electric double layer forming at the solid–liquid interface has a complex internal structure consisting of a Stern layer and a diffuse layer with a resulting complex refractive index profile which is related to the density profile (Fig. 2b). The ellipsometric measurement captures only the net integrated effect of this profile. Hence, we represent the entire electric double layer by a single adsorbed layer with an effective refractive index $n_a$ and an effective thickness $d_a$ (Fig. 2c), following the standard approach (see *e.g.* [29]). Below, we will discuss some limitations of this approach regarding the interpretation of the data in terms of simultaneously adsorbed counter-ions and depleted co-ions.

The measured AOI dependent $\Psi$ and $\Delta$ curves are fitted by adjusting the values of $n_a$ and $d_a$, as well as the bulk refractive index $n_{bulk}$. Fitting of the $\Psi$, $\Delta$ curves is carried out using the commercial software EP4 (Accurion).

In dynamic (*i.e.* time dependent) adsorption measurements, the AOI is fixed at the value where $\Psi$ is found to be minimal, *i.e.* 51° in our experiments with the silica exposed to pure water. A measurement then consists of a continuous recording of $\Psi$ and $\Delta$ as a function of time, while solutions are flushed through the microfluidic channels at typical flow rates of order of 1 μL/min. Each recording of a ($\Psi$, $\Delta$) data point takes approximately 9 s. All measurements were carried out in a temperature controlled room ($22 \pm 1$ °C). The thickness of the bare silica layer is measured at the beginning and at the end of the experiment for each sample. It is typically found to vary by less than ±0.1 nm. This indicates that neither dissolution of the silica layer nor permanent adsorption play an important role in these measurements.

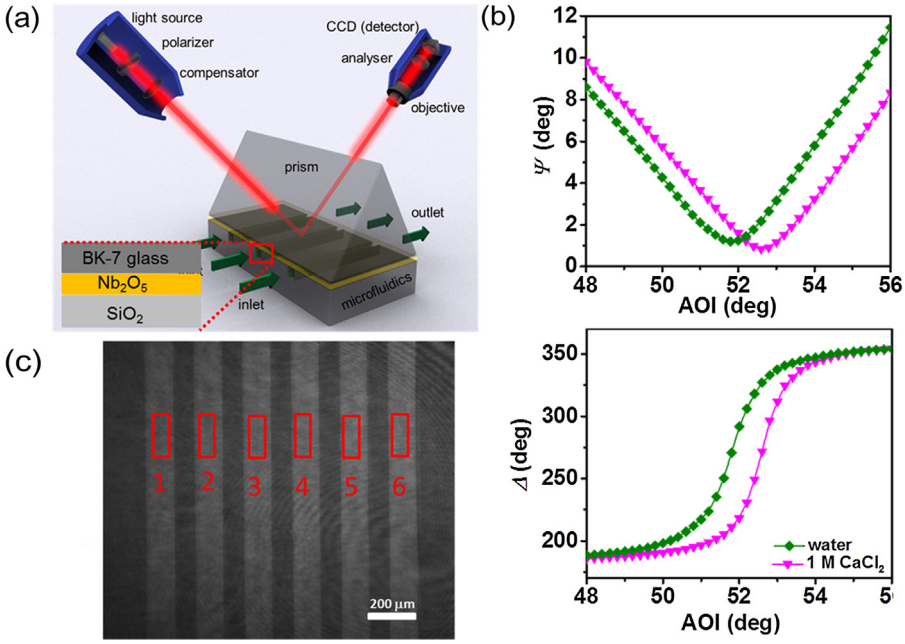


**Fig. 1.** (a) Central part of the IRE setup, equipped with a microfluidic cell. The silica-coated BK7/$Nb_2O_5$ substrate is directly attached to the prism with index matching oil. Fluids with adsorbing species are flushed through microfluidic channels, having the silica sensor surface as their ceiling; (b) a typical IRE measurement showing the ellipsometric angles $\Psi$ (top) and $\Delta$ (bottom) *vs.* the angle of incidence (AOI): with water (olive diamonds) and 1 M $CaCl_2$ solution (magenta triangles) in the flow cell, solid lines guide the eye; (c) 6 parallel channels in the field of view. Light gray areas correspond to the channels filled with solution; the dark areas show the PDMS walls. (For interpretation of the references to color in this figure legend, the reader is referred to the web version of this article.)

## 3. Results and discussion

To demonstrate the strength and sensitivity of the technique, we studied the adsorption of ions to solid–liquid interfaces. As a well-characterized system, we select aqueous solutions of NaCl, $CaCl_2$ and silica surfaces. The adsorption behavior of both salts was studied while tuning the surface charge of the silica *via* the pH. At pH 3, silica surfaces are essentially uncharged because this is close to the point of zero charge [30]. At pH 10, the silanol groups are largely deprotonated and the silica surface carries a negative charge [31]. To compensate this charge, cations need to adsorb to the interfaces.

Experimental data of $\Psi$ and $\Delta$ *vs.* AOI for a variety of $CaCl_2$ solutions at the two pH values studied under quasi-static conditions are displayed in Fig. 3. In Fig. 4 dynamic (*i.e.* time dependent) adsorption measurements for water and 0.5 M $CaCl_2$ at two pH conditions are shown. In the latter measurements, $\Psi$ and $\Delta$ are continuously recorded as a function of time, keeping the AOI fixed, while solutions are flushed through the microfluidic channels. In the present work, where ions are the adsorbing species, the typical timescale of the adsorption process is (much) shorter than the time resolution of our setup. So we only show the measurement at equilibrium conditions as displayed by the plateaus in Fig. 4. Similar results are obtained for NaCl and $CaCl_2$ solutions with concentrations ranging from 0.01 M to 1 M (data not shown).

Variations of ellipsometric angle shifts *vs.* AOI or time when flushing with 'pure' (without additional salt) water at pH 3 and 10 are indistinguishable, *i.e.* the addition of 0.1 M HCl or NaOH to vary the pH has a negligible effect on the refractive index of the

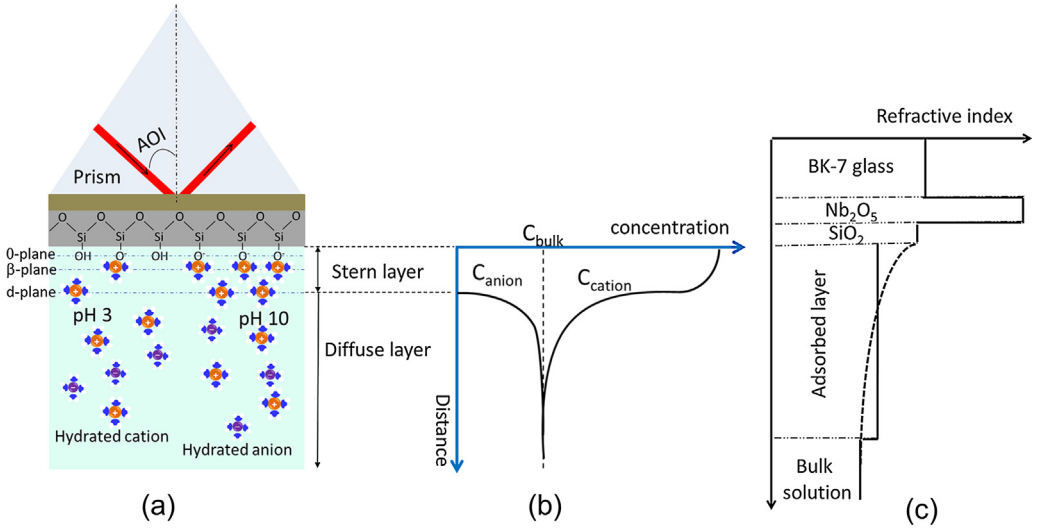


**Fig. 2.** (a) Schematic illustration of laser path inside the prism (BK-7 glass) and the electric double layer (EDL); (b) distribution of cations and anions in EDL; (c) refractive index profile used in the analysis of IRE measurement: the dashed line representing the EDL is modeled as an effectively homogeneous layer.

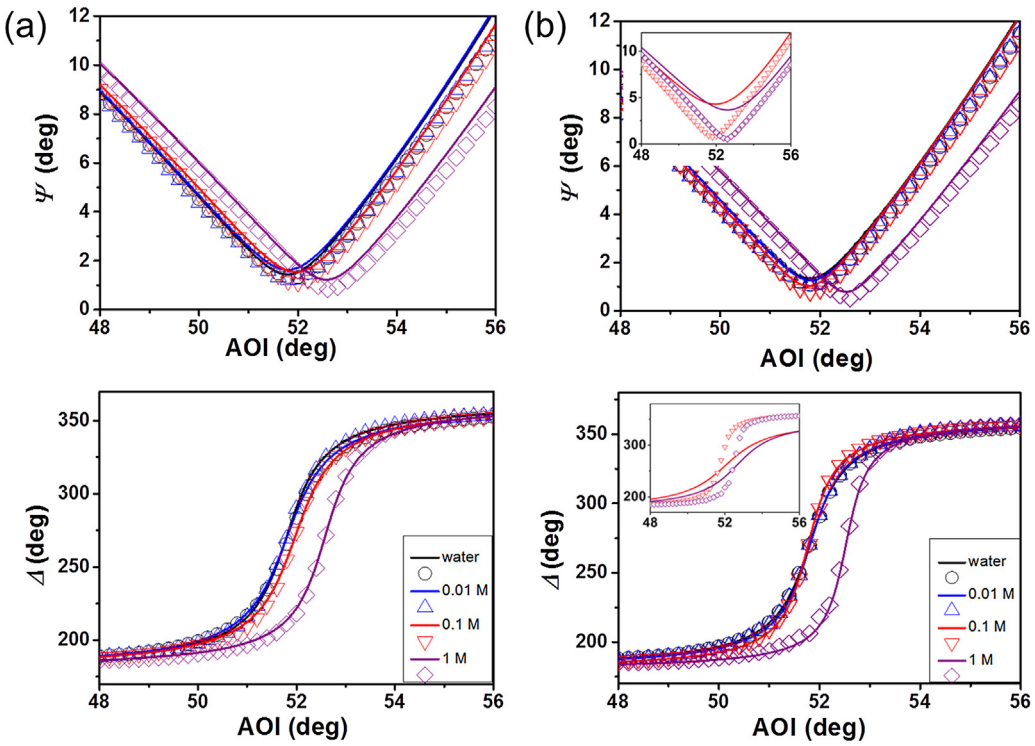


**Fig. 3.** Ellipsometric angles $\Psi$ and $\Delta$ as a function of angle of incidence (AOI) for various concentrations of $CaCl_2$ at pH 3 (a) and pH 10 (b). Symbols are the experimental data, and solid lines are calculations from a layer stack model. For (a) and the inset in (b), we used a four-layer model including the 1st, 2nd, 3rd and 5th layer in Table 1, leaving $n_{bulk}$ as a fitting parameter. For the main panel of (b), we used a model which includes all five layers in Table 1, assuming $d_a$ as 0.5 nm and leaving $n_a$, $n_{bulk}$ as fitting parameters.

solutions below the detection limit of our instrument. This is especially clear in Fig. 4, where solutions at both pH conditions are flushed and results are displayed in the same graph. Because the pH induced variations of the surface charge alone remain undetected, the observed variations of the signals in Figs. 3 and 4 must be caused by the added salt. The $\Delta$ angle shifts are larger than those of $\Psi$. For pH 3, the shifts in $\Psi$ and $\Delta$ can be fitted quantitatively by assuming variations of the bulk refractive index $n_{bulk}$, with the 4-layer model: BK-7 glass → $Nb_2O_5$ → $SiO_2$ → bulk solution (Fig. 3a). The extracted $n_{bulk}$ values are the same as measured independently by a refractometer (Fig. 5). Fig. 4 also shows that the adsorption and desorption processes are perfectly reversible within the resolution of our experiment.

This result is consistent with the general picture that silica–water interfaces at pH 3 are uncharged and the adsorption of ions thus negligible. At pH 10, however, following the same approach to fit the shifts of $\Psi$ and $\Delta$ observed is no longer possible (see insets of Fig. 3b). To fit the pH 10 data, we need to add one additional layer representing the electric double layer to the optical model. We leave $n_a$ and $n_{bulk}$ as fitting parameters, $d_a$ is fixed at 0.5 nm. As expected, the extracted values of $n_{bulk}$ turn out to be consistent with the values measured with the refractometer and also correspond well to the data for pH 3, see Fig. 5. This justifies use of the five-layer stack model at pH 10. Fitted curves of other salt solutions look similar to those in Fig. 3.

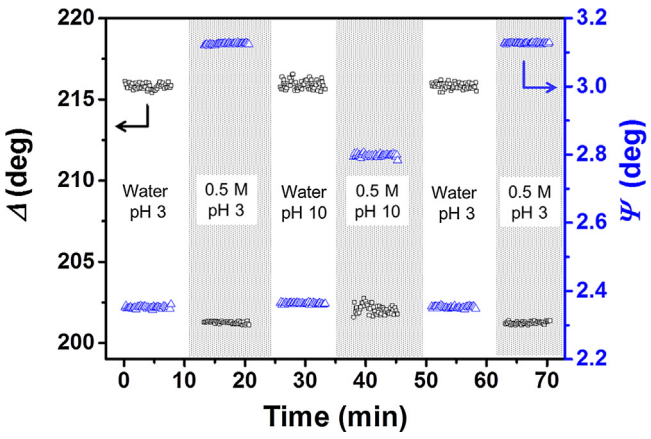


**Fig. 4.** Time dependent IRE measurement: $\Delta$ and $\Psi$ angle shifts upon consecutive flushing water and 0.5 M $CaCl_2$ (aq) at pH 3 and pH 10. Only the data obtained after reaching equilibrium are shown.

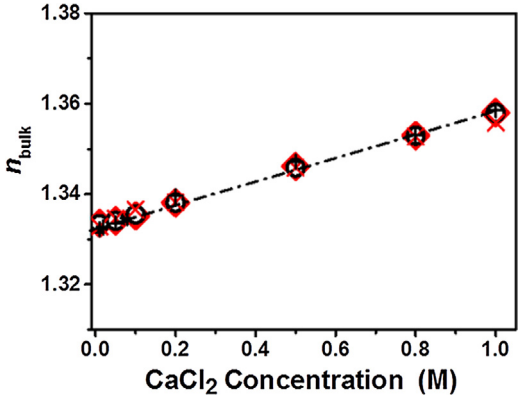


**Fig. 5.** Comparison between refractive index values of $CaCl_2$ solutions: extracted from modeling (cross, with the layer stack model used in Fig. 3 for pH 3 and 10, respectively) and measured with refractometer (open square and circle). Black is at pH 10, and red is at pH 3. (For interpretation of the references to color in this figure legend, the reader is referred to the web version of this article.)

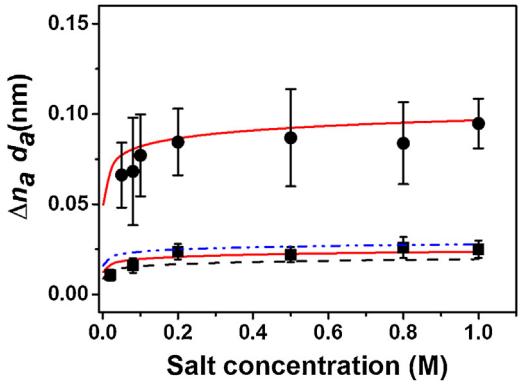


**Fig. 6.** Optical thickness of NaCl (square) and $CaCl_2$ (circle) *vs.* the salt concentration at pH 10. The solid symbols are the experimental results and the lines are the calculations from surface complexation model. For NaCl, three $pK_{Na}$ values are used: 2.65 (blue dash dot line), 1.65 (red solid line) and 0.65 (black dash line). (For interpretation of the references to color in this figure legend, the reader is referred to the web version of this article.)

As noted above, the resulting optical parameters $n_a$ and $d_a$ of the adsorption layer are effective values that represent the actual refractive index profile. Following de Feijter et al. [29] we can express them as:

$$n_a = \frac{\int n(z)(n(z) - n_{\text{bulk}})\,\mathrm{d}z}{\int (n(z) - n_{\text{bulk}})\,\mathrm{d}z} \tag{1}$$

and

$$d_a = \frac{1}{n_a - n_{\text{bulk}}} \int (n(z) - n_{\text{bulk}})\,\mathrm{d}z \tag{2}$$

where the integrals extend from zero to infinity, *i.e.* from the surface into the bulk liquid. Upon fitting the 5 layer stack model to the experimental data, it turns out that the values obtained for $n_a$ and $d_a$ are highly correlated. Fits of similar quality can be obtained for 0.5 nm < $d_a$ < 5 nm and $n_a$ varying in such a manner that the excess optical thickness $\Delta n_a d_a = (n_a - n_{\text{bulk}})\,d_a$ due to the ion adsorption remains essentially constant, *i.e.* independent of the choice of $d_a$. We find values $\Delta n_a d_a \ll 1$ nm for all experimental conditions. For such small values, it is well-known that ellipsometry does not provide a reliable distinction between refractive index and thickness [28,32,33]. Fig. 6 shows that $\Delta n_a d_a$ increases with increasing (cation) concentration for both NaCl and $CaCl_2$ at pH 10. The excess optical thickness for the $CaCl_2$ salt exceeds the one for NaCl by approximately a factor four, indicating a much stronger adsorption for the divalent salts. For pH 3 the excess optical thickness is found to be zero within experimental error for both salts at all concentrations (data not shown).

To relate the measured excess optical thickness to the physical surface excess of adsorbed ions, we express the local refractive index $n(z)$ of the salt solution in terms of the local excess concentration $\Delta c_i(z) = c_i(z) - c_{i,\text{bulk}}$ for each ionic species $i$, as caused by adsorption and depletion (see Fig. 2b).

$$n(z) = n_{\text{bulk}} + \sum_i \alpha_i \Delta c_i(z)\,. \tag{3}$$

Here, the sum runs over all species in the solution, *i.e.* the anions and cations in our case. The coefficients $\alpha_i = \mathrm{d}n/\mathrm{d}c_i$ indicate the increment of the refractive index with increasing concentration of species $i$. Combining these equations with the standard definition for the surface excess for each species

$$\Gamma_i = \int \Delta c_i(z)\,\mathrm{d}z \tag{4}$$

we can write

$$\Delta n_a \quad d_a = \sum_i \alpha_i \quad \Gamma_i. \tag{5}$$

where $\Delta n_a = L^{-1} \int_0^L (n(z) - n_{\text{bulk}})\,\mathrm{d}z$, with an arbitrary normalization thickness $L \gg d_a$. The excess optical thickness of the adsorption layer thus has a direct physical meaning and expresses the combined surface excess of all ions in the solution, each weighted by its refractive index increment $\alpha_i$. For the specific case of our salt solutions, Eq. (5) simplifies to

$$\Delta n_a \quad d_a = \alpha_+ \Gamma_+ + \alpha_- \Gamma_- = \alpha_+ \left(\Gamma_+ - \frac{1}{z}\Gamma\right) + \frac{\mathrm{d}n}{\mathrm{d}c}\frac{1}{z}\Gamma \tag{6}$$

where $\Gamma_{+/-}$ and $\alpha_{+/-}$ denote the excess and the refractive index increment of the cations and anions, $z$ is the valence of cations and $\mathrm{d}n/\mathrm{d}c$ is the bulk increment of the refractive index upon adding salt, which is known experimentally. For NaCl and $CaCl_2$, we use $\mathrm{d}n/\mathrm{d}c\big|_{\text{NaCl}} = 10.17$ mL/mol and $\mathrm{d}n/\mathrm{d}c\big|_{\text{CaCl}_2} = 23.59$ mL/mol. Moreover, we use $\alpha_{\text{Na}^+} = 7.1$ mL/mol, $\alpha_{\text{Ca}^{2+}} = 17.59$ mL/mol, as reported by Porus et al. [21].

To compare our experimental results to a model, we calculate the expected surface excess using the standard triple layer model of the electric double layer [20,34]. Coupling the Poisson–Boltzmann theory for the diffuse layer to surface complexation reactions [35,36] including the equilibrium constants as specified in Table 2, we can calculate the expected surface excess $\Gamma_i$ for each ionic species, as shown in Fig. 7. The solid lines in Fig. 6 show that the resulting model predictions are in good agreement with the experimental data. To illustrate the level of sensitivity, we also plot two competing lines for NaCl adsorption assuming $pK_{Na}$ values one unit higher and lower than reported in Refs. [37,38]. The resulting dashed and dotted lines in Fig. 6 are still compatible with the experimental data, indicating the range of uncertainty in the analysis.

Given the reasonable agreement between model and experimental data, we explore the consequences of the surface complexation model in more detail. In Fig. 7, we plot the excess of cations and anions for the Stern layer and the diffuse layer separately. Again, we only show the data for pH 10 because adsorption at pH 3 is negligible. As expected, a strong positive excess is found for the counter ions (*i.e.* the cations) in the Stern layer. Simultaneously, there is, however, a positive excess of counter ions and depletion (negative excess) of co-ions from the diffuse layer, too. All excesses display a finite dependence on the salt concentration for concentrations below approximately 0.2 M and saturate for higher concentrations. Multiplying each excess with the corresponding refractive index increment, we find that the optical thickness shown in Fig. 6 is dominated by the contribution from the Stern layer, as concluded earlier by Porus et al. [25]. Yet, the contribution of the diffuse layer is not negligible and amounts to approximately 15% of the total excess of ions.

From Fig. 7, we also conclude that the total adsorption of $Ca^{2+}$ (*i.e.* $-SiO^-\ Ca^{2+}$ and $-SiO^-(CaOH)^+$ species together) to the surface is much more pronounced than the adsorption of $Na^+$. According to the model this contribution is largely caused by the strong adsorption of $CaOH^+$ with its rather high p$K$ value. This strong adsorption implies an enhanced Ca-induced deprotonation of silanol groups, which is required to preserve overall charge neutrality.

The use of the Poisson Boltzmann theory in combination with surface complexation models has been criticized (see [44] for an extensive discussion). In particular for divalent cations such as $Ca^{2+}$ at elevated concentrations, extensions of the Poisson Boltzmann theory that take into account lateral interactions with the adsorbed layer, *e.g.* due to the finite volume of the ions, electrostatic and hydrogen bonding interactions (see *e.g.* [45]) are generally relevant.

**Table 2**
Surface complexation reactions and parameters used in triple layer model.

| | Surface complexation reactions | Equilibrium constant, $K_i$ (mol/L) | Capacitance (F/m$^2$) [20,34,39] | |
|---|---|---|---|---|
| | | | $C_1$ | $C_2$ |
| H | $\equiv SiOH \leftrightarrow \equiv SiO^- + H^+$ | $10^{-6.9}$ [20,40,41] | | |
| NaCl | $\equiv SiO^- Na^+ \leftrightarrow \equiv SiO^- + Na^+$ | $10^{-1.65}$ [37,38,41] | 1.0 | 0.2 |
| $CaCl_2$ | $\equiv SiO^- Ca^{2+} \leftrightarrow \equiv SiO^- + Ca^{2+}$ | $10^{-0.7}$ | 1.4 | 0.2 |
| | $\equiv SiO^-(CaOH)^+ + H^+ \leftrightarrow \equiv SiO^- + Ca^{2+} + H_2O$ [39,42,43] | $10^{8.2}$ | | |
| Site Density (nm$^{-2}$): 8.0 [40] | | | | |

*Note:* The site density is the surface concentration of silanol surface groups, indicating the maximum number of sites that can get deprotonated.

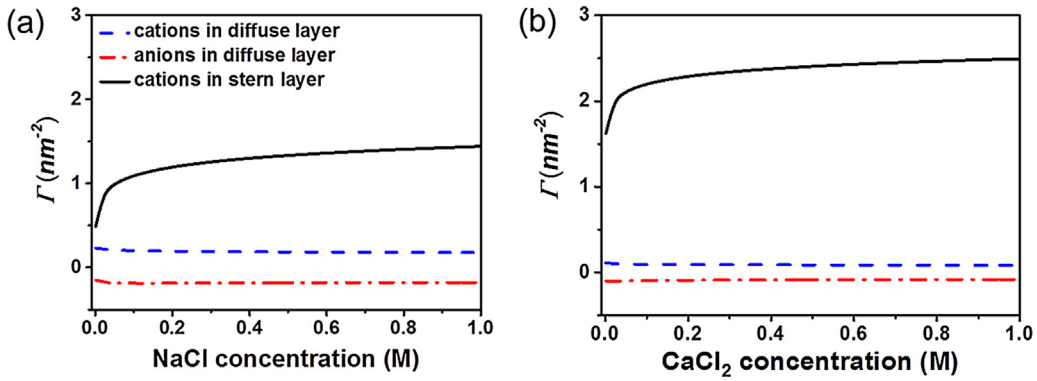


**Fig. 7.** Calculation of Surface excess of cations in stern layer (black line), cations in diffuse layer (blue dash line), and anions in diffuse layer (red dash dot line) from surface complexation model as a function of NaCl (a) and $CaCl_2$ (b) concentrations at pH 10. (For interpretation of the references to color in this figure legend, the reader is referred to the web version of this article.)

Porus et al. [21] argue that any mean field theory is inadequate to study such systems. Recent work on $Ca^{2+}$ adsorption on gibbsite using a combination of high resolution atomic force microscopy and density functional theory [25] also suggests a high degree of complexity exceeding the present surface complexation analysis. Nevertheless, the latter provides a reasonable description of the adsorption data presented here that is consistent with various other earlier potentiometric titration [46–48]. The data presented in this work are insufficient to provide strong arguments in favor of any of the competing models. Possibly our results could be equally explained in terms of ion correlations, as in Ref. [21].

To disprove either of the theories, it would be important to design experiments that can be described by one approach but not by others. Next to a broader set of experimental data this will probably require the combination of several complementary probes, including perhaps optical spectroscopies to detect beyond doubt the presence of certain species at the interface. Another interesting option is the combination of optical measurements (like the present one) and force measurements. While the latter ones probe the total charge in the diffuse layer, the former ones – as the present experiments suggest – only probe cations from the salt but not protons and hydroxyl ions. Exploring this complementarity in a single experiment is expected to provide additional insights. Optical experiments in combination with microfluidics that allow for a high degree of parallelization as demonstrated here are expected to offer a pathway to the required rapid screening of large parameter spaces of fluid compositions.

## 4. Conclusion

We presented a sensitive optical technique – internal reflection ellipsometry – for probing adsorption at liquid–solid interfaces in combination with microfluidic channels. The sensitivity of this technique is demonstrated by its ability to detect adsorption and depletion of monovalent and divalent salt ions at silica–water interfaces under various pH conditions. The adsorption and desorption reactions are found to be perfectly reversible. The measured excess optical thickness of adsorbed ions is linked to the Gibbs surface excess of each ion species. The presented adsorption isotherms are successfully modeled using a mean field Poisson Boltzmann theory in combination with a triple layer surface complexation model. We anticipate that the combination with more sophisticated microfluidics device will enable efficient high speed screening of adsorption/desorption processes for a wide range of applications.

## Acknowledgements

We acknowledge D. Wijnperlé, D. Hagedoorn and A. Pit for the design and preparation of the microfluidics. We also acknowledge Prof. Dr. M.A. Cohen Stuart for fruitful discussions. Financial support was provided through the Exploratory Research (ExploRe) program of BP plc.

## Appendix A. Supplementary data

Supplementary data associated with this article can be found, in the online version, at http://dx.doi.org/10.1016/j.snb.2014.12.127.

## References

[1] B.C. Donose, I.U. Vakarelski, K. Higashitani, Silica surfaces lubrication by hydrated cations adsorption from electrolyte solutions, Langmuir 21 (2005) 1834–1839.
[2] V.J. Inglezakis, S.G. Poulopoulos, Adsorption, Ion Exchange and Catalysis, Elsevier, The Netherlands, 2006.
[3] Kasper Wenderich, A. Klaassen, Igor Siretanu, Frieder Mugele, Guido Mul, Sorption determined deposition of Pt on well-defined plate-like WO3, Angew. Chem. Int. Ed. (2014), 10.1002/anie.201405274R1 and 10.1002/ange.201405274R1.
[4] R. Nasralla, H. Nasr-El-Din, SPE Asia Pacific Oil and Gas Conference and Exhibition, 2011.

[5] K. Kataoka, A. Harada, Y. Nagasaki, Block copolymer micelles for drug delivery: design, characterization and biological significance, Adv. Drug Delivery Rev. 47 (2001) 113–131.
[6] D. Mohan, C.U. Pittman Jr., Arsenic removal from water/wastewater using adsorbents—a critical review, J. Hazard. Mater. 142 (2007) 1–53.
[7] A.M. Brzozowska, M.H.G. Duits, F. Mugele, Stability of stearic acid monolayers on artificial sea water, Colloids Surf., A: Physicochem. Eng. Aspects 407 (2012) 38–48.
[8] N. Kumar, L. Wang, I. Siretanu, M. Duits, F. Mugele, Salt dependent stability of stearic acid Langmuir–Blodgett films exposed to aqueous electrolytes, Langmuir 29 (2013) 5150–5159.
[9] X. Wang, S.Y. Lee, K. Miller, R. Welbourn, I. Stocker, S. Clarke, M. Casford, P. Gutfreund, M.W.A. Skoda, Cation bridging studied by specular neutron reflection, Langmuir 29 (2013) 5520–5527.
[10] F. Mugele, I. Siretanu, N. Kumar, B. Bera, L. Wang, A. Maestro, M. Duits, D. van den Ende, I. Collins, in: Society of Petroleum Engineers Source SPE Improved Oil Recovery Symposium, 12-16 April, Tulsa, Oklahoma, USA, Soc. Pet. Eng. (2014), http://dx.doi.org/10.2118/169143-MS, Document ID SPE-169143-MS, ISBN 978-1-61399-309-5.
[11] A.M. Brzozowska, F. Mugele, M.H.G. Duits, Stability and interactions in mixed monolayers of fatty acid derivatives on artificial sea water, Colloids Surf., A: Physicochem. Eng. Aspects 433 (2013) 200–211.
[12] R. De Ruiter, R.W. Tjerkstra, M.H.G. Duits, F. Mugele, Influence of cationic composition and pH on the formation of metal stearates at oil–water interfaces, Langmuir 27 (2011) 8738–8747.
[13] A. Lager, K. Webb, C. Black, M. Singleton, K. Sorbie, Low salinity oil recovery—an experimental investigation, Petrophysics 49 (2008) 28.
[14] T. Hassenkam, J. Mathiesen, C. Pedersen, K. Dalby, S. Stipp, I.R. Collins, SPE Improved Oil Recovery Symposium, Society of Petroleum Engineers, 2012.
[15] J. Seccombe, A. Lager, G. Jerauld, B. Jhaveri, T. Buikema, S. Bassler, J. Denis, K. Webb, A. Cockin, E. Fueg, SPE Improved Oil Recovery Symposium, Society of Petroleum Engineers, 2010.
[16] A. Muggeridge, A. Cockin, K. Webb, H. Frampton, I. Collins, T. Moulds, P. Salino, Recovery rates, enhanced oil recovery and technological limits, Philos. Trans. R. Soc. Ser. A: Math. Phys. Eng. Sci. 373 (2035) (2014) 1–25.
[17] J.J. Lyklema, Fundamentals of Interface and Colloid Science: Solid–Liquid Interfaces, vol. 2, Elsevier, Amsterdam, 1995, pp. 4.2.
[18] G.A. Parks, P.L. De Bruyn, The zero point of charge of oxides, J. Phys. Chem. 66 (1962) 967–973.
[19] A.V. Delgado, F. González-Caballero, R.J. Hunter, L.K. Koopal, J. Lyklema, Measurement and interpretation of electrokinetic phenomena, J. Colloid Interface Sci. 309 (2007) 194–224.
[20] J.A. Davis, R.O. James, J.O. Leckie, Surface ionization and complexation at the oxide/water interface: I. Computation of electrical double layer properties in simple electrolytes, J. Colloid Interface Sci. 63 (1978) 480–499.
[21] M. Porus, C. Labbez, P. Maroni, M. Borkovec, Adsorption of monovalent and divalent cations on planar water–silica interfaces studied by optical reflectivity and Monte Carlo simulations, J. Chem. Phys. 135 (2011) 064701.
[22] C. Labbez, B. Jönsson, M. Skarba, M. Borkovec, Ion–ion correlation and charge reversal at titrating solid interfaces, Langmuir 25 (2009) 7209–7213.
[23] A. Rimola, D. Costa, M. Sodupe, J.-F. Lambert, P. Ugliengo, Silica surface features and their role in the adsorption of biomolecules: computational modeling and experiments, Chem. Rev. 113 (2013) 4216–4313.
[24] P. Koelsch, H. Motschmann, A method for direct determination of the prevailing counterion distribution at a charged surface, J. Phys. Chem. B 108 (2004) 18659–18664.
[25] M. Porus, P. Maroni, M. Borkovec, Highly-sensitive reflectometry setup capable of probing the electrical double layer on silica, Sens. Actuators B: Chem. 151 (2010) 250–255.
[26] M. Ricci, P. Spijker, F. Stellacci, J.-F. Molinari, K. Voïtchovsky, Direct visualization of single ions in the stern layer of calcite, Langmuir 29 (2013) 2207–2216.
[27] I. Siretanu, D. Ebeling, M.P. Andersson, S.S. Stipp, A. Philipse, M.C. Stuart, D. van den Ende, F. Mugele, Direct observation of ionic structure at solid–liquid interfaces: a deep look into the Stern layer, Sci. Rep. 4 (2014) 1–7.
[28] H. Tompkins, E.A. Irene, Handbook of Ellipsometry, William Andrew, Norwich, 2005.
[29] J.A. de Feijter, J. Benjamins, F.A. Veer, Ellipsometry as a tool to study the adsorption behavior of synthetic and biopolymers at the air–water interface, Biopolymers 17 (1978) 1759–1772.
[30] M. Kosmulski, The pH-dependent surface charging and the points of zero charge, J. Colloid Interface Sci. 253 (2002) 77–87.
[31] H. Horiuchi, A. Nikolov, D.T. Wasan, Calculation of the surface potential and surface charge density by measurement of the three-phase contact angle, J. Colloid Interface Sci. 385 (2012) 218–224.
[32] F.L. McCrackin, E. Passaglia, R.R. Stromberg, H.L. Steinberg, Measurement of the thickness and refractive index of very thin films and the optical properties of surfaces by ellipsometry, J. Res. Nat. Bur. Sect. A 67 (1963) 363.
[33] A. Piegari, E. Masetti, Thin film thickness measurement: a comparison of various techniques, Thin Solid Films 124 (1985) 249–257.
[34] J.A. Davis, J.O. Leckie, Surface ionization and complexation at the oxide/water interface II. Surface properties of amorphous iron oxyhydroxide and adsorption of metal ions, J. Colloid Interface Sci. 67 (1978) 90–107.
[35] D.E. Yates, T.W. Healy, The structure of the silica/electrolyte interface, J. Colloid Interface Sci. 55 (1976) 9–19.
[36] A. Kitamura, K. Fujiwara, T. Yamamoto, S. Nishikawa, H. Moriyama, Analysis of adsorption behavior of cations onto quartz surface by electrical double-layer model, J. Nucl. Sci. Technol. 36 (1999) 1167–1175.
[37] N. Sahai, D.A. Sverjensky, Solvation and electrostatic model for specific electrolyte adsorption, Geochim. Cosmochim. Acta 61 (1997) 2827–2848.
[38] N. Sahai, D.A. Sverjensky, Evaluation of internally consistent parameters for the triple-layer model by the systematic analysis of oxide surface titration data, Geochim. Cosmochim. Acta 61 (1997) 2801–2826.
[39] D.A. Sverjensky, Interpretation and prediction of triple-layer model capacitances and the structure of the oxide–electrolyte–water interface, Geochim. Cosmochim. Acta 65 (2001) 3643–3655.
[40] T. Hiemstra, W.H. Van Riemsdijk, G.H. Bolt, Multisite proton adsorption modeling at the solid/solution interface of (hydr)oxides: a new approach: I. Model description and evaluation of intrinsic reaction constants, J. Colloid Interface Sci. 133 (1989) 91–104.
[41] Cunlu Zhao, D. E., Siretanu I., H.T.M. van den Ende, Mugele F. Extracting local surface charges and ion adsorption characteristics from atomic force microscopy measurements at solid–electrolyte interfaces. (in preparation).
[42] S.A. Greenberg, The chemisorption of calcium hydroxide by silica, J. Phys. Chem. 60 (1956) 325–330.
[43] R.O. James, T.W. Healy, Adsorption of hydrolyzable metal ions at the oxide–water interface. III. A thermodynamic model of adsorption, J. Colloid Interface Sci. 40 (1972) 65–81.
[44] J. Lyklema, Molecular interpretation of electrokinetic potentials, Curr. Opin. Colloid Interface Sci. 15 (2010) 125–130.
[45] D. Ben-Yaakov, D. Andelman, D. Harries, R. Podgornik, Beyond standard Poisson–Boltzmann theory: ion-specific interactions in aqueous solutions, J. Phys.: Condens. Matter 21 (2009) 424106.
[46] M. Kobayashi, M. Skarba, P. Galletto, D. Cakara, M. Borkovec, Effects of heat treatment on the aggregation and charging of Stöber-type silica, J. Colloid Interface Sci. 292 (2005) 139–147.
[47] P.M. Dove, C.M. Craven, Surface charge density on silica in alkali and alkaline earth chloride electrolyte solutions, Geochim. Cosmochim. Acta 69 (2005) 4963–4970.
[48] T.F. Tadros, J. Lyklema, Adsorption of potential-determining ions at the silica–aqueous electrolyte interface and the role of some cations, J. Electroanal. Chem. Interfacial Electrochem. 17 (1968) 267–275.

## Biographies

**Lei Wang** obtained her diploma in physical chemistry in 2011 at Shandong University, China. Currently she is studying adsorption–desorption of organic/inorganic molecules at solid–liquid interfaces as a Ph.D. student in University of Twente, The Netherlands.

**Cunlu Zhao** obtained his Bachelor and Master degrees at Xi'an Jiaotong University (China) in 2004 and 2007, respectively. Later, he continued the study at Nanyang Technological University (Singapore) where he obtained the Ph.D. degree in 2012. Now he works as a postdoctoral research fellow at University of Twente. His research interests include electro-thermo-kinetics, transport phenomena at micro/nano scales, soft matter mechanics, renewable energy *etc.*

**Michel H.G. Duits** obtained his M.Sc. and Ph.D. degrees in Utrecht, with a specialization in physical chemistry. Since 1991 he has been working at the University of Twente in the Rheology and later in Physics of Complex fluids group. His fields of interests are colloids, interfacial layers, rheology, microscopy and microfluidics. He has supervised 15 Ph.D. students/postDocs and published 60 papers in international refereed journals.

**Frieder Mugele** obtained his diploma in physics at the University of Konstanz (Germany). Since 2004, he holds the chair of the Physics of Complex Fluids at the University of Twente. His current research interests are concentrated in the areas of micro/nanofluidics and confinement effects, (electro-)wetting, and also enhanced oil recovery. He has co-authored >130 research papers and so far, 17 Ph.D. projects were successfully completed under his auspices.

**Igor Siretanu** obtained his B.Ed. and M.sc. Degrees in theoretical physics at Moldova State University in 2005 and 2007, respectively. He has received his PhD. degree in 2011 in physical chemistry at University of Bordeaux 1, France. Since 2012 he is a postdoctoral researcher at the University of Twente. His current research interests focus on fundamental force interactions with high-resolution AFM at surface from the nanometer to the atomic scale.